Eur Radiol
DOI 10.1007/s00330-015-4101-9

NEURO

Quantitative validation of a visual rating scale for frontal atrophy: associations with clinical status, APOE e4, CSF biomarkers and cognition

Daniel Ferreira[1] · Lena Cavallin[2,3] · Tobias Granberg[2,3] · Olof Lindberg[1] · Carlos Aguilar[1] · Patrizia Mecocci[4] · Bruno Vellas[5] · Magda Tsolaki[6] · Iwona Kłoszewska[7] · Hilkka Soininen[8] · Simon Lovestone[9] · Andrew Simmons[10,11,12] · Lars-Olof Wahlund[1] · Eric Westman[1] · for the AddNeuroMed consortium and for the Alzheimer's Disease Neuroimaging Initiative

Received: 3 September 2015 / Revised: 14 October 2015 / Accepted: 30 October 2015

Abstract

Objectives To validate a visual rating scale of frontal atrophy with quantitative imaging and study its association with clinical status, APOE ε4, CSF biomarkers, and cognition.

Methods The AddNeuroMed and ADNI cohorts were combined giving a total of 329 healthy controls, 421 mild cognitive impairment patients, and 286 Alzheimer's disease (AD) patients. Thirty-four patients with frontotemporal dementia (FTD) were also included. Frontal atrophy was assessed with the frontal sub-scale of the global cortical atrophy scale (GCA-F) on T1-weighted images. Automated imaging markers of cortical volume, thickness, and surface area were evaluated. Manual tracing was also performed.

Results The GCA-F scale reliably reflects frontal atrophy, with orbitofrontal, dorsolateral, and motor cortices being the regions contributing most to the GCA-F ratings. GCA-F primarily reflects reductions in cortical volume and thickness, although it was able to detect reductions in surface area too. The scale showed significant associations with clinical status and cognition.

Conclusion The GCA-F scale may have implications for clinical practice as supportive diagnostic tool for disorders

* Data used in preparation of this article were obtained from the Alzheimer's Disease Neuroimaging Initiative (ADNI) database (adni.loni.usc.edu). As such the investigators within the ADNI contributed to the design and implementation of ADNI and/or provided data but did not participate in analysis or writing of this report. A complete listing of ADNI investigators can be found at: http://adni.loni.usc.edu/wp-content/uploads/how_to_apply/ADNI_Acknowledgement_List.pdf.

✉ Daniel Ferreira
daniel.ferreira.padilla@ki.se

1 Division of Clinical Geriatrics, Center for Alzheimer Research, Department of Neurobiology, Care Sciences and Society, Karolinska Institutet, Novum, 5th floor, SE-141 86 Stockholm, Sweden

2 Division of Medical Imaging and Technology, Department of Clinical Science, Intervention and Technology, Karolinska Institutet, Stockholm, Sweden

3 Department of Radiology, Karolinska University Hospital in Huddinge, Huddinge, Sweden

4 Institute of Gerontology and Geriatrics, University of Perugia, Perugia, Italy

5 INSERM U 558, University of Toulouse, Toulouse, France

6 3rd Department of Neurology, Aristoteleion Panepistimeion Thessalonikis, Thessaloniki, Greece

7 Medical University of Lodz, Lodz, Poland

8 University of Eastern Finland, University Hospital of Kuopio, Kuopio, Finland

9 Department of Psychiatry, Warneford Hospital, University of Oxford, Oxford, UK

10 Department of Neuroimaging, Institute of Psychiatry, King's College London, London, UK

11 NIHR Biomedical Research Centre for Mental Health, London, UK

12 NIHR Biomedical Research Unit for Dementia, London, UK

Published online: 11 November 2015

demonstrating predominant frontal atrophy such as FTD and the executive presentation of AD. We believe that GCA-F is feasible for use in clinical routine for the radiological assessment of dementia and other disorders.

Key points

- *The GCA-F visual rating scale reliably reflects frontal brain atrophy.*
- *Orbitofrontal, dorsolateral, and motor cortices are the most contributing regions.*
- *GCA-F shows significant associations with clinical status and cognition.*
- *GCA-F may be supportive diagnostic tool for disorders demonstrating predominant frontal atrophy.*
- *GCA-F may be feasible for use in radiological routine.*

Keywords Frontal atrophy · Neuroimaging · Alzheimer's disease · Mild cognitive impairment · Frontotemporal dementia

Abbreviations

MTA	medial temporal atrophy
PA	posterior atrophy
GCA	global cortical atrophy
GCA-F	global cortical atrophy – frontal sub-scale
SFG	superior frontal gyrus
MFG	middle frontal gyrus
IFG	inferior frontal gyrus
ORB	orbitofrontal cortex
DACC	and dorsal anterior cingulate gyrus

Introduction

Different clinical presentations of Alzheimer's disease (AD) are now recognized in the current diagnostic criteria [1]. The amnestic presentation is most common and depicts the typical phenotype of AD characterized by cognitive impairment in episodic memory. The other presentations are non-amnestic in their origin and their diagnosis is often challenging. Since neurodegeneration can be studied with imaging techniques, visual rating scales of regional atrophy may be valuable to support diagnosis of different AD presentations. Their advantage over automated methods is that they are already used in clinical work, can be implemented both in magnetic resonance and computerized tomography images (even in different protocols and quality), and are quick and easy to use. The medial temporal atrophy (MTA) scale [2] has been incorporated in the diagnostic algorithm of AD to assess hippocampal atrophy [1, 3], and shows a well-established association with the amnestic presentation [2, 4–6]. The posterior atrophy (PA) scale [7] has proved useful in cases with atrophy in the parietal and occipital lobes [8], and may thus be useful for the visuospatial and language presentations. Given that executive dysfunction has been extensively associated with atrophy in the frontal lobe [9], a visual rating scale of frontal atrophy may support diagnosis of the executive AD presentation. However, no visual rating scales of frontal atrophy have been specifically validated for AD to date. Since the global cortical atrophy (GCA) scale [10, 11] includes a separate assessment of the frontal lobe (i.e., GCA-F), and has been extensively applied in AD [11–18], it could serve as a framework for assessing frontal atrophy. Such a scale may also be of value for other disorders with predominant frontal atrophy such as frontotemporal dementia (FTD).

In the current study we provide a comprehensive validation of the GCA-F scale using quantitative imaging as previously done for other visual rating scales [19–21]. Three different levels of anatomical detail were covered by performing analyses of the entire frontal lobe, the individual frontal subregions, and the whole cortical mantle providing a much finer analysis at the vertex level. We also analyzed three different markers of brain integrity, i.e., cortical volume, cortical thickness, and cortical surface area, and assessed which frontal subregions contributed most to the discrimination between GCA-F scores. Fully automated methods were used in a large sample including AD, MCI, and healthy control subjects, and gold standard manual tracings were used in a smaller sample including patients with FTD. Finally, we studied the association between GCA-F and clinical status, cerebrospinal (CSF) biomarkers, and cognition.

Materials and methods

Subjects

Data from AddNeuroMed and ADNI studies were combined providing a total of 1036 individuals: healthy controls (n=329), mild cognitive impairment (MCI) (n=421), and AD (n=286). AddNeuroMed is part of the InnoMed European Union FP6 programme and was designed to develop and validate surrogate markers in AD [22]. ADNI was launched in 2003 by the National Institute on Aging, the National Institute of Biomedical Imaging and Bioengineering, the Food and Drug Administration, private pharmaceutical companies, and non-profit organizations [23]. The project was established to develop standardized imaging techniques and biomarkers in AD research. Data were obtained from the ADNI database (adni.loni.usc.edu, PI Michael M. Weiner). Participant recruitment and eligibility criteria were very similar in both cohorts [22, 24].

In addition, thirty-four patients with FTD were enrolled from a previous study [25] in order to test the GCA-F scale in a disorder typically displaying atrophy in the frontal lobe. Briefly, this cohort included patients with the behavioural

variant of FTD (bvFTD, n=12), progressive non-fluent aphasia (PNFA, n=9), and semantic dementia (SD, n=13). Patients were recruited from the Memory Clinic at Karolinska University Hospital Huddinge, Stockholm, Sweden. Clinical diagnoses were determined on multidisciplinary consensus according to Neary et al. criteria [26]. Further details are provided elsewhere [25]. The study was approved by the Regional Ethical Review Board in Stockholm, Sweden.

Magnetic resonance imaging and visual rating of frontal atrophy

A 3D T1-weighted MPRAGE sequence was acquired in the three samples, AddNeuroMed, ADNI, and the Memory Clinic [22, 25, 27]. The GCA scale was applied in axial plane, restricting the original criteria from Pasquier et al. [10] to the frontal lobe in order to provide a measurement of frontal atrophy (i.e., GCA-F). Scores range from 0 (no atrophy) to 3 (end-stage degree of atrophy) (details in Fig. 1). Intra-rater x(L.C.) and inter-rater (L.C. and T.G.) reliability were tested in 100 randomly selected participants, providing weighted kappa values of 0.70 and 0.59, respectively. Intraclass correlation coefficients showed averaged absolute agreement of 0.79. L.C. has 8 years of experience using GCA and T.G. is newly trained. Both raters were blind to diagnosis, demographic, and clinical information.

Automated reconstruction and parcellation of the cortex, performed in AddNeuroMed and ADNI samples

Cortical reconstruction was performed using FreeSurfer 5.3.0 (http://surfer.nmr.mgh.harvard.edu/) (see Appendix Table 6 for full details and references). This procedure provides measurements of cortical volume, cortical thickness, and cortical surface area for 34 regions for each hemisphere, as well as a measurement of the total intracranial volume (TIV). Frontal regions were combined to provide four functional-anatomical relevant sub-regions, also reducing the number of multiple comparisons: dorsolateral, medial, motor, and orbitofrontal cortices (Fig. 2). In addition, a measurement of the entire frontal lobe was calculated by combining the four frontal sub-regions (i.e., frontal ROI).

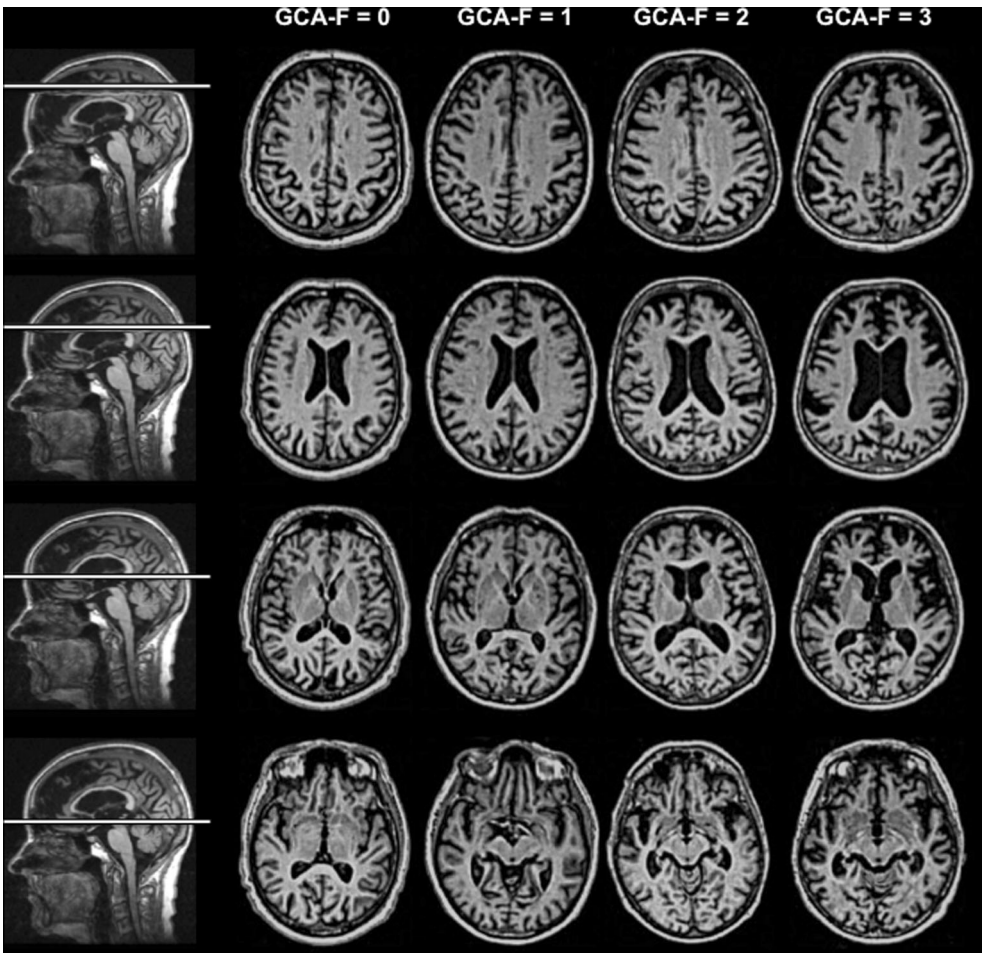

Fig. 1 Scoring of the visual rating scale for frontal atrophy (GCA-F). The GCA scale was applied to axial T1-weighted images, restricting the original criteria from Pasquier et al. [10] to the frontal lobe in order to provide a measurement of frontal atrophy (i.e., GCA-F). Briefly, sulcal dilatation is determined as absent (GCA-F=0), mild (GCA-F=1), moderate (GCA-F=2), or severe (GCA-F=3). Clear guidelines for determining sulcal dilatation are provided in Pasquier et al. [10]. The anatomical boundaries of the frontal lobe were defined by the central sulcus at the posterior part, the frontal bone at the anterior and dorsal parts, and the fissure of Sylvius at the ventral posterior part. Ratings were performed on axial reconstructions

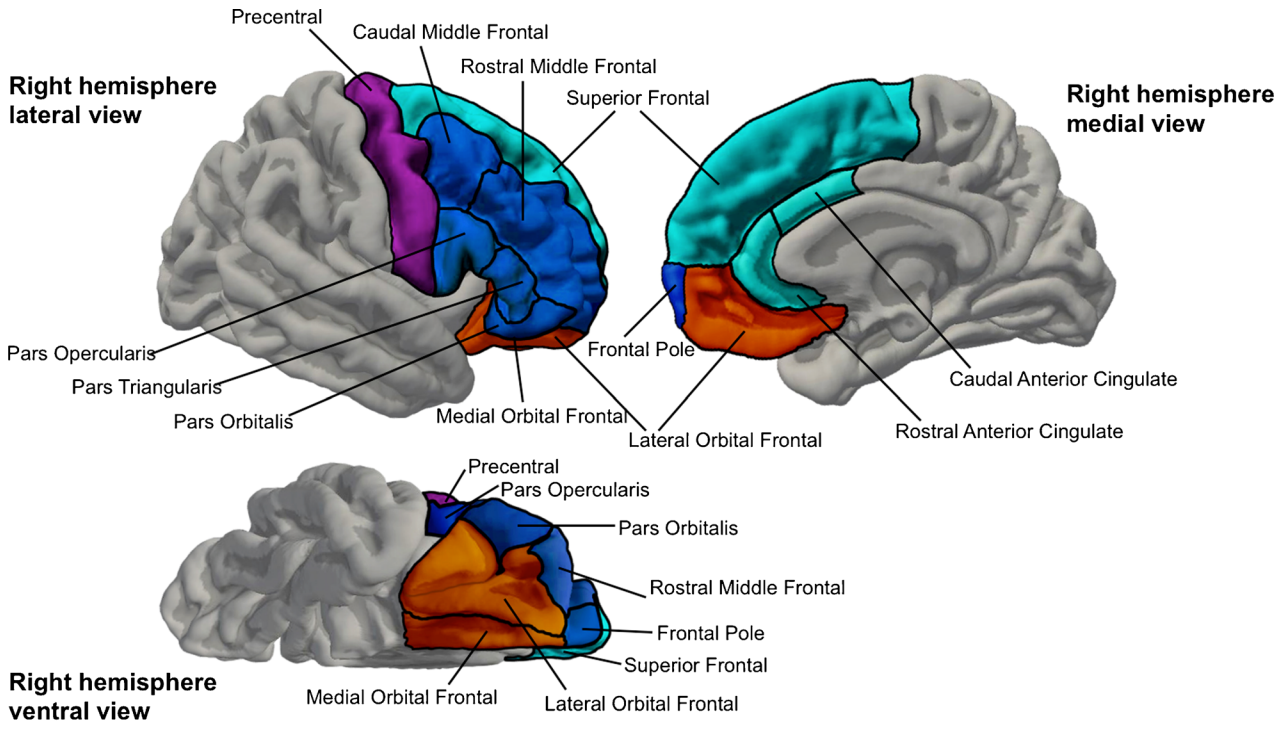

Frontal ROI = **DORSOLATERAL CORTEX** (caudal middle frontal + rostral middle frontal + pars opercularis + pars triangularis + pars orbitalis + frontal pole) + **MEDIAL CORTEX** (superior frontal + rostral anterior cingulate + caudal anterior cingulate) + **MOTOR CORTEX** (precentral) + **ORBITOFRONTAL CORTEX** (lateral orbital frontal + medial orbital frontal)

Fig. 2 Cortical parcellation and calculation of the frontal ROI and frontal sub-regions. FreeSurfer 5.3.0 parcellates the cortical surface in to 34 regions for each hemisphere. Regions of the frontal lobe were combined to provide four frontal sub-regions: dorsolateral cortex (also including ventrolateral cortex), medial cortex, motor cortex, and orbitofrontal cortex. The superior frontal gyrus was assigned to the medial cortex since most of this area is displayed in the medial part of the frontal lobe. In addition, a measurement of the entire frontal lobe was calculated by combining the four frontal sub-regions (i.e., frontal ROI). Values of cortical volume, cortical thickness, and cortical surface area are available for all the regions. Non-frontal regions are displayed in gray

Manual tracing of frontal sub-regions, performed in the Memory Clinic sample

Volumetric values for the FTD patients including the following frontal regions (left and right) and the TIV were taken from our previous study [25]: superior frontal gyrus (SFG), middle frontal gyrus (MFG), inferior frontal gyrus (IFG), orbitofrontal cortex (ORB), and dorsal anterior cingulate gyrus (DACC). Methods for manual tracing and volume calculation are fully described elsewhere [25] and in Appendix Table 7.

Clinical status, CSF biomarkers, and cognitive variables

Procedures for assessing clinical status, CSF biomarkers, and cognitive performance are described elsewhere [24, 28]. Clinical status was assessed with MMSE, CDR, GDS, FAQ, and APOE ε4 status. CSF levels of $A\beta_{1-42}$, total tau (T-tau) and phosphorylated tau (p-tau) were also studied. The following cognitive tests were included: trail making test (TMT), digit symbol, digit span, semantic fluency (animals), auditory verbal learning test (AVLT), Boston naming test (BNT), and clock test.

Statistical analysis

One-way independent ANOVA/ANCOVA was used for continuous variables and the Chi-square test for dichotomous variables. Mixed ANCOVA was used to analyze the interaction between two or more independent variables. Following previous studies [19], age and gender were not included as covariates because the GCA-F rating was blind to this information. Binary logistic regression was performed to assess which frontal sub-regions contributed most to a higher score on GCA-F. The *P*-values in all principal and post-hoc analyses were adjusted using Bonferroni correction for multiple comparisons. Results were considered significant when $p \leq 0.05$. Analyses were performed using SPSS 22.0 for Mac.

Vertex analyses across the cortical mantle were conducted using FreeSurfer software. A general linear model was fitted

at each vertex using cortical volume, thickness, or area as dependent variables. Results were tested against an empirical null distribution of maximum cluster size across 5.000 iterations. Z Monte Carlo simulations were used with a cluster-forming threshold of $p \leq 0.05$ (two-sided), yielding clusters corrected for multiple comparisons across the cortical mantle.

Results

Table 1 shows the demographics. Patients with bvFTD and PNFA evidenced the greatest degree of frontal atrophy as measured by the GCA-F scale, followed by the AD and MCI groups (Fig. 3). Since asymmetry is key finding in FTD, the GCA-F scale was also applied separately to the two hemispheres in the FTD patients. Interestingly, a significant interaction between FTD subtype and hemisphere was found ($F_{(2,\ 31)}=5.512$; $p=0.009$) (Appendix Fig. 5). BvFTD patients had qualitatively more frontal atrophy in the right hemisphere, PNFA patients had qualitatively more frontal atrophy in the left hemisphere, and there were no between-hemispheric differences in SD patients.

All the participants were then classified according to their GCA-F ratings for the validation analyses. The three patients rated as GCA-F=3 (one AD, one bvFTD, and one PNFA) were added to the GCA-F=2 group in order to provide three large GCA-F groups. Demographics for these three groups are displayed in Appendix Table 8.

Association of GCA-F with automated imaging

These analyses were performed only in AddNeuroMed and ADNI samples. ANCOVA performed at the frontal ROI level showed that higher scores in GCA-F were associated with smaller volume ($F_{(2,\ 1032)}=85.163$; $p<0.001$), thickness ($F_{(2,\ 1032)}=90.338$; $p<0.001$), and area ($F_{(2,\ 1032)}=13.738$; $p<0.001$) (Table 2).

Several mixed ANCOVA were performed to study the interaction between GCA-F group (between-subjects factor), frontal sub-region (within-subjects factor), and hemisphere (within-subjects factor). Interactions involving hemispheres by GCA-F group were not significant. Therefore, measures from left and right hemispheres were combined and a new mixed ANCOVA was performed for the GCA-F group and the frontal sub-region. Results showed significant interactions between the GCA-F group and the frontal sub-region for the three markers: volume ($F_{(4.843,\ 2498.848)}=41.163$; $p<0.001$); thickness ($F_{(4.344,\ 2241.461)}=5.712$; $p<0.001$), and area ($F_{(4.273,\ 2204.665)}=8.550$; $p<0.001$). Regarding volume, there were significant differences among the three GCA-F groups in all frontal sub-regions, but the magnitude of the difference was smaller in motor cortex ($\eta_p^2=0.04$), than in the other three regions ($\eta_p^2 \geq 0.12$) (Table 2). Regarding thickness, there were significant differences among the three GCA-F groups in all frontal sub-regions, but the magnitude of the difference was smaller in the medial and motor cortices ($\eta_p^2=0.05$), than in the dorsolateral and orbitofrontal cortices ($\eta_p^2=0.15$) (Table 2). Finally, results for area showed that GCA-F had a significant effect in all frontal sub-regions except the motor cortex. Moreover, there were significant differences among the three GCA-F groups only in the the dorsolateral cortex. For both medial and orbitofrontal cortices, there were significant differences only between GCA-F=2 and the other two GCA-F groups, but not between GCA-F=0 and GCA-F=1 (Table 2).

Analyses at the vertex level showed that higher scores in GCA-F were associated with less volume and cortical thickness in the whole frontal lobe. Results showed larger significant clusters when comparing GCA-F=0 vs. GCA-F=1 than when comparing GCA-F=1 vs. GCA-F=2 (Fig. 4 and Appendix Table 9). Higher GCA-F scores were also associated with smaller surface area but to a lesser extent as compared with volume and cortical thickness. In addition, higher GCA-F scores showed a significant association with smaller volume, thickness, and area in several temporal and posterior areas.

Logistic regression analyses showed that different frontal sub-regions contributed to the GCA-F ratings depending on the marker considered (Table 3). Regarding volume, dorsolateral cortex was the only region that contributed statistical

Table 1 Demographic characteristics and GCA-F across clinical groups

	HC	MCI	AD	bvFTD	PNFA	SD	*p*
Group size, n	329	421	286	12	9	13	-
Age, mean (Sd)	75.0 (5.8)	74.9 (6.7)	75.8 (6.9)	59.5 (6.9) [a,b,c]	64.9 (7.2) [a,b,c]	63.8 (7.1) [a,b,c]	<0.001
Gender, % female	50	39 [a]	55 [b]	75	67	62	<0.001
Years of education, mean (Sd) [1]	14.2 (4.4)	13.8 (4.6)	12.0 (4.9) [a,b]	12.4 (3.8)	8.0 (1.2) [a]	10.5 (2.7)	<0.001
GCA-F score, mean (Sd)	0.40 (0.56)	0.57 (0.65) [a]	0.81 (0.73) [a,b]	1.67 (0.78) [a,b,c]	1.44 (0.73) [a,b]	0.15 (0.38) [c,d,e]	<0.001

[1] $n=1061$ (missing cases: 1 MCI, 2 AD, 2 bvFTD, 4 PNFA); [a] Significantly different from CTRL; [b] Significantly different from MCI; [c] Significantly different from AD; [d] Significantly different from bvFTD; [e] Significantly different from PNFA; Bonferroni correction for three comparisons: $p \leq 0.017$; All post-hoc analyses were also adjusted using Bonferroni correction for multiple comparisons; GCA-F=global cerebral atrophy – frontal sub-scale; Sd=standard deviation; HC=healthy controls; MCI=mild cognitive impairment; AD=Alzheimer's disease; bvFTD=behavioural variant of frontotemporal dementia; SD=semantic dementia; PNFA=progressive non-fluent aphasia

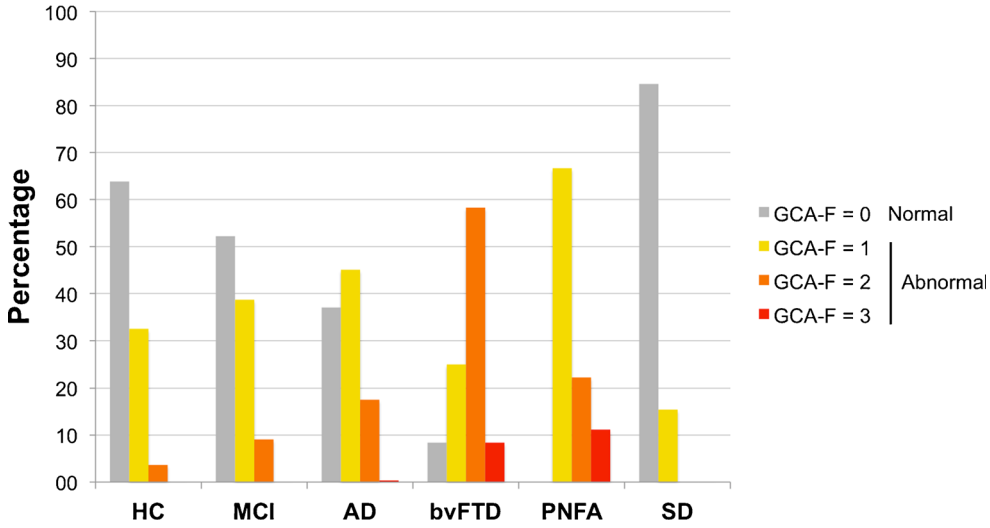

Fig. 3 GCA-F scores across clinical groups. Bars represent percentage of cases with a given GCA-F score within each diagnostic group. GCA-F=0 is considered normal, and GCA-F≥ 1 is considered abnormal according to a previously proposed cut-off [18]. GCA-F= global cerebral atrophy – frontal sub-scale; HC=healthy controls; MCI=mild cognitive impairment; AD=Alzheimer's disease; bvFTD=behavioural variant of frontotemporal dementia; SD= semantic dementia; PNFA= progressive non-fluent aphasia

significance to the discrimination between GCA-F=0 and GCA-F=1 (ß=-0.198), and orbitofrontal cortex to the discrimination between GCA-F=1 and GCA-F=2 (ß=-0.265). Regarding thickness, dorsolateral cortex (ß=-0.674), orbitofrontal cortex (ß=-0.443), and motor cortex (ß= 0.282), were the regions that contributed statistically significantly to the discrimination between GCA-F=0 and GCA-F=1, and orbitofrontal cortex to the discrimination between GCA-F=1 and GCA-F=2 (ß=-0.610). Regarding area, motor cortex was the only region that contributed statistically significantly to the discrimination between GCA-F=0 and GCA-F=1 (ß=0.210).

Table 2 Association of GCA-F with automated imaging: frontal ROI and frontal sub-regions (AddNeuroMed+ADNI)

	GCA-F=0 (*N*=536)	GCA-F=1 (*N*=399)	GCA-F=2 (*N*=101)	*p*	η_p^2
Frontal ROI					
Volume, mm^3	141111 (15277)	135054 (16251) [a]	127489 (17140) [a,b]	<0.001	0.14
Area, mm^2	55126 (5578)	54567 (6035) [a]	53260 (6139) [a,b]	<0.001	0.03
Thickness, mm	2.39 (0.13)	2.31 (0.13) [a]	2.23 (0.14) [a,b]	<0.001	0.15
Dorsolateral					
Volume, mm^3	52936 (6366)	50348 (6557) [a]	47386 (7134) [a,b]	<0.001	0.14
Area, mm^2	21279 (2413)	20964 (2518) [a]	20441 (2702) [a,b]	<0.001	0.02
Thickness, mm	2.30 (0.14)	2.20 (0.14) [a]	2.12 (0.15) [a,b]	<0.001	0.15
Medial					
Volume, mm^3	43658 (5067)	41818 (5323) [a]	39299 (5689) [a,b]	<0.001	0.12
Area, mm^2	15725 (1737)	15569 (1938)	15126 (1921) [a,b]	<0.001	0.02
Thickness, mm	2.58 (0.16)	2.52 (0.17) [a]	2.46 (0.19) [a,b]	<0.001	0.05
Orbitofrontal					
Volume, mm^3	21453 (2283)	20611 (2395) [a]	19430 (2547) [a,b]	<0.001	0.12
Area, mm^2	8379 (887)	8295 (923)	8064 (943) [a,b]	<0.001	0.02
Thickness, mm	2.36 (0.14)	2.26 (0.15) [a]	2.17 (0.17) [a,b]	<0.001	0.15
Motor					
Volume, mm^3	21469 (2685)	20784 (2950) [a]	19986 (2768) [a,b]	<0.001	0.04
Area, mm^2	9284 (935)	9295 (1033)	9195 (959)	0.428	0
Thickness, mm	2.18 (0.20)	2.11 (0.20) [a]	2.05 (0.17) [a,b]	<0.001	0.05

[a] Significantly different from GCA-F=0; [b] Significantly different from GCA-F=1; Values in the table represent mean (standard deviation); TIV was included as covariate in all analyses except for dorsolateral thickness and motor thickness, where one-way independent ANOVA was performed since these two measures showed no significant correlation with TIV (dorsolateral: r=-0.036, p=0.247; motor: r=0.018, p=0.567); Bonferroni correction for three comparisons (ANCOVA for frontal ROI): $p \leq 0.017$; Bonferroni correction for twelve comparisons (ANOVA/ANCOVA for frontal sub-regions): $p \leq 0.004$; All post-hoc analyses were also adjusted using Bonferroni correction for multiple comparisons; GCA-F=global cerebral atrophy – frontal sub-scale; ROI=region of interest; mm=millimetres; η_p^2 =partial eta squared

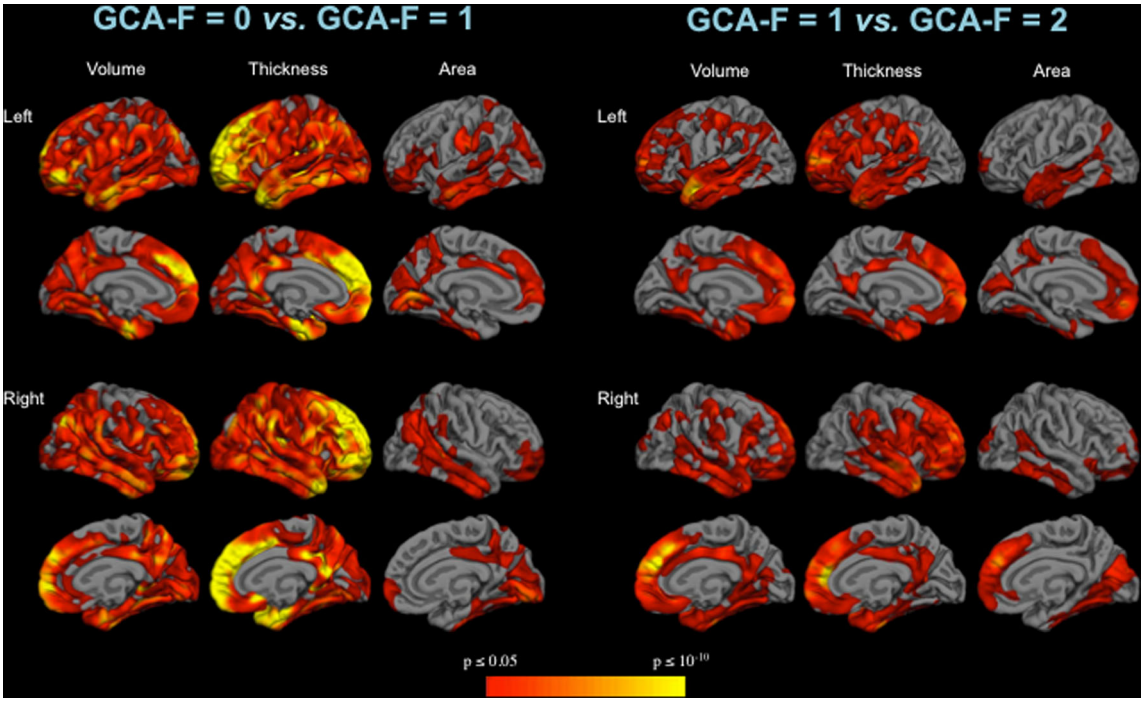

Fig. 4 Association of GCA-F and automated imaging: analysis at the vertex level (AddNeuroMed+ADNI). Vertex analyses across the cortical mantle were conducted using FreeSurfer software. Maps were smoothed using a circularly symmetric Gaussian kernel across the surface with a full width at half maximum (FWHM) of 10 mm. A general linear model was fitted at each vertex. GCA-F group was entered as independent variable (GCA-F=0 *vs.* GCA-F=1; and GCA-F=1 *vs.* GCA-F=2), with TIV entered as a covariate. Z Monte Carlo simulations were conducted for cluster-forming with a threshold of $p \leq 0.05$ (two-sided), yielding clusters corrected for multiple comparisons across the cortical mantle. Only vertexes belonging to clusters surviving this correction are displayed. Significant clusters arising from the comparison between GCA-F groups were mapped on standard templates, depicted in lateral (first and third rows) and medial (second and fourth rows) views, both for left and right hemispheres. The coloured regions illustrate less cortical volume, cortical thickness, or cortical surface area in the group with higher GCA-F score. The coloured bar illustrates the significance level of the differences from red ($p \leq 0.05$) to yellow ($p \leq 10^{-10}$). GCA-F=global cerebral atrophy – frontal sub-scale

Association of GCA-F with manual tracing

These analyses were performed only in the Memory Clinic sample (FTD patients). Higher scores in GCA-F were associated with smaller volume in all the manually traced frontal sub-regions (bilateral SFG and ORB, left IFG, and right MFG and DACC, see Table 4).

Association of GCA-F with clinical status, CSF biomarkers, and cognition

Regarding AddNeuroMed and ADNI samples, higher GCA-F scores were associated with worse clinical status (MMSE, CDR, and FAQ), but not with depressive symptomatology (GDS) and presence of the APOE ε4 allele (Table 5). There was no significant association between GCA-F and CSF $A\beta_{1\text{-}42}$, T-tau, and p-tau. Regarding cognitive variables, higher GCA-F scores were associated with worse cognitive performance in TMT, digit symbol, semantic fluency, AVLT learning, AVLT delayed, BNT, and clock test. Effect sizes revealed that GCA-F had a larger effect on TMT-B, digit symbol, and AVLT learning.

Regarding the sample from the Memory Clinic (FTD patients), no significant association was found between GCA-F scores and MMSE ($F_{(2, 31)}=1.228$; $p=0.308$) (Table 5).

Discussion

This study shows that the GCA-F scale reliably reflects frontal atrophy in several clinical groups (i.e., AD, MCI, and FTD) as well as in healthy controls. The orbitofrontal, dorsolateral, and motor cortices were the regions contributing most to the GCA-F ratings. The scale primarily reflects reductions in volume and cortical thickness, although it was able to reflect reductions in surface area as well. Finally, the scale showed significant associations with clinical status and cognition.

Providing a visual rating scale of frontal atrophy for AD is important. Such a scale may also be valuable for other disorders with predominant frontal atrophy.

Table 3 Regional contribution to the GCA-F ratings (AddNeuroMed+ADNI)

Marker	Model				Predictors					
DV (X)	χ^2	*p*	R^2_N	%	IV (Y)	*p*	ß	SE	Exp(B)	95 % CI
Volume										
GCA-F=0 *vs*. GCA-F=1	8.521	0.004	0.012	57.3	Dorsolateral	0.004	-0.198	0.068	0.821	0.718 – 0.938
					Medial	0.604				
					Orbitofrontal	0.887				
					Motor	0.093				
GCA-F=1 *vs*. GCA-F=2	5.848	0.016	0.018	79.8	Dorsolateral	0.823				
					Medial	0.813				
					Orbitofrontal	0.017	-0.265	0.111	0.767	0.617 – 0.953
					Motor	0.284				
Area										
GCA-F=0 *vs*. GCA-F=1	10.026	0.002	0.014	59.0	Dorsolateral	0.083				
					Medial	0.554				
					Orbitofrontal	0.543				
					Motor	0.002	0.210	0.067	1.234	1.083 – 1.407
GCA-F=1 *vs*. GCA-F=2		*ns*.			Dorsolateral	0.735				
					Medial	0.867				
					Orbitofrontal	0.937				
					Motor	0.272				
Thickness										
GCA-F=0 *vs*. GCA-F=1	5.969	0.015	0.167	65.3	Dorsolateral	<0.001	-0.674	0.153	0.510	0.378 – 0.689
					Medial	0.326				
					Orbitofrontal	<0.001	-0.443	0.112	0.642	0.516 – 0.799
					Motor	0.015	0.282	0.117	1.326	1.055 – 1.667
GCA-F=1 *vs*. GCA-F=2	28.184	<0.001	0.086	80.0	Dorsolateral	0.076				
					Medial	0.803				
					Orbitofrontal	<0.001	-0.610	0.120	0.543	0.429 – 0.687
					Motor	0.837				

Binary logistic regression analysis. GCA-F groups were entered as dependent variables, in two conditions: GCA-F=0 vs. GCA-F=1; and GCA-F=1 vs. GCA-F=2; Values of cortical volume, thickness, and area of the four frontal sub-regions were transformed to z-scores and included as independent variables; the forward likelihood ratio method was used; Exp(B) is an indicator of the change in odds resulting from a unit change in the predictor: values greater than one indicate that as the predictor increases, the odd of the outcome occurring increases, and values lesser than one indicate that as the predictor increases, the odds of the outcome occurring decrease; DV=dependent variable; IV=independent variable; GCA-F=global cerebral atrophy – frontal sub-scale; R^2_N=Negelkerke's adjusted R squared; SE=standard error; 95 % CI=95 % confidence interval; ns. = non-significant

Although some approaches have been reported in the previous literature, they are not specific for the frontal lobe and are not validated for AD [21, 29, 30]. On the contrary, the global cortical atrophy (GCA) scale [10, 11], has been extensively applied in AD [11–18]. Three previous studies specifically assessed frontal atrophy in AD based on GCA-F [11, 14, 18]. Scheltens et al. showed that GCA-F was the GCA sub-scale with the best inter-observer agreement [11]. Doody et al. showed that GCA-F was not correlated with APOE ε4 status [14]. We proposed a list of practical cut-offs for GCA-F, MTA, and PA, and demonstrated that their combination increases accuracy in AD diagnosis and prediction of progression from MCI to AD [18]. However, GCA-F had not been quantitatively validated to date.

In this study we show that GCA-F reliably reflects cortical atrophy in the frontal lobe at three levels of anatomical detail: the entire frontal lobe, specific frontal sub-regions, and at the vertex level across the cortical mantle. The orbitofrontal, dorsolateral, and motor cortices were the regions that contributed the most to the GCA-F ratings in AD, MCI, and healthy control groups. This finding was also confirmed in the FTD sample, especially for the

Table 4 Association of GCA-F with manual tracing (Memory Clinic)

	GCA-F=0 (*N*=12)	GCA-F=1 (*N*=11)	GCA-F=2 (*N*=11)	*p*	η_p^2
L SFG	1.708 (0.283)	1.589 (0.221)	1.408 (0.192) [a]	0.017	0.23
R SFG	1.823 (0.166)	1.644 (0.253)	1.406 (0.253) [a]	0.001	0.39
L MFG	1.133 (0.190)	1.058 (0.141)	0.955 (0.187)	0.066	0.16
R MFG	1.128 (0.201)	1.055 (0.119)	0.868 (0.084) [a,b]	0.001	0.38
L IFG	0.682 (0.112)	0.774 (0.131)	0.583 (0.121) [b]	0.004	0.31
R IFG	0.650 (0.093)	0.669 (0.131)	0.615 (0.175)	0.646	0.03
L ORB	0.938 (0.094)	0.940 (0.073)	0.762 (0.081) [a,b]	<0.001	0.52
R ORB	0.923 (0.095)	0.923 (0.083)	0.760 (0.134) [a,b]	0.001	0.36
L DACC	0.128 (0.033)	0.121 (0.020)	0.110 (0.029)	0.334	0.07
R DACC	0.124 (0.022)	0.163 (0.033) [a]	0.129 (0.017) [b]	0.001	0.34

[a] Significantly different from GCA-F=0; [b] Significantly different from GCA-F=1; Values in the table represent mean (standard deviation); All volumetric values are divided by total intracranial volume (TIV) and multiplied by 100; Bonferroni correction for ten comparisons: $p \leq 0.005$; All post-hoc analyses were also adjusted using Bonferroni correction for multiple comparisons; GCA-F=global cerebral atrophy – frontal sub-scale; L=left; R=right; SFG=superior frontal gyrus; MFG=middle frontal gyrus; IFG=inferior frontal gyrus; ORB=orbitofrontal cortex; DACC=dorsal anterior cingulate cortex; η_p^2 =partial eta squared

superior part of the dorsolateral cortex and the orbitofrontal region. Since the frontal lobe is large, this information is important for potential simplification of the GCA-F scale, as well as to guide radiologists to specific anatomical landmarks, and to know which regions are less well captured by the GCA-F scale. Analyses at the vertex level complemented these results showing significant associations also with temporal and posterior cortices. A possible explanation for this is that GCA-F primarily reflects frontal atrophy, but since this finding occurs in the context of a more global pattern of AD-related atrophy [18], the scale also reflects atrophy in other key regions for AD. This finding was supported by the pattern of associations with clinical and cognitive variables. Although effect sizes revealed that GCA-F had a larger effect on TMT-B and digit symbol (two executive tasks), as well as AVLT learning (a memory task with high involvement of the frontal lobe during the learning phase [31]), higher GCA-F scores were also associated with cognitive measures involving episodic memory (AVLT delayed and recognition), semantic fluency, naming (BNT), and visuoconstructive skills (clock test), primarily associated with temporal and posterior cortices; as well as global clinical impairment (MMSE, CDR, FAQ).

Different markers of brain integrity were analyzed in this study. Volume measures were included as in previous validation studies [19–21]. Since cortical volume is a product of cortical thickness and surface area, these two markers were also assessed in order to further understand differences in volume. Higher GCA-F scores were associated with less cortical volume, primarily explained by differences in thickness but also in area to a lesser extent. This finding is important for the clinical applicability of GCA-F given that different neurodevelopmental and neurodegenerative disorders have a differential impact on the cerebral cortex. Reductions in thickness but not area have been described in AD, Parkinson's disease, and multiple sclerosis [32–34]; reductions in area but not thickness have been reported in Williams syndrome [35]; and reductions in both thickness and area have been found in schizophrenia [36]. Our results support the generic applicability of GCA-F. Results obtained in the FTD sample also support the use of GCA-F in disorders displaying an asymmetric patter of frontal atrophy. The GCA-F results in this study strongly correspond with what previously demonstrated using quantitative imaging in the same FTD sample [25] and other studies [37]. The GCA-F scale also captured greater frontal atrophy in FTD than in AD, as previously described using quantitative imaging [38–40].

The main strengths of this study are the inclusion of the largest cohort to date for the validation of a visual rating scale of frontal atrophy; the application of an advanced automated imaging technique and gold standard manual tracing; analysis of association with clinical status, CSF biomarkers, and cognition; and the inclusion of different disorders. Some limitations should also be discussed. We observed a ceiling effect on the GCA-F scores especially in the healthy controls, MCI, and SD groups, where perhaps more fine-grained techniques might be needed in order to capture very subtle atrophy. The only three individuals rated GCA-F=3 were added to the group of GCA-F=2 in order to provide three large severity groups. Despite this slightly reduced scale range, comparison between GCA-F=0 and GCA-F=1 is clinically relevant because abnormality is determined by GCA-F scores ≥1 [18]. Comparison between GCA-F=1

Table 5 Association of GCA-F with clinical status, CSF biomarkers, and cognitive impairment

	N	GCA-F=0	GCA-F=1	GCA-F=2	*p*	η_p^2
AddNeuroMed+ADNI						
Clinical variables						
MMSE	1020	27.2 (2.9)	25.9 (3.8) [a]	24.3 (4.1) [a,b]	<0.001	0.07
CDR	1022	0.4 (0.3)	0.5 (0.5) [a]	0.7 (0.5) [a,b]	<0.001	0.07
GDS	1023	2.1 (2.2)	2.3 (2.4)	2.2 (2.4)	0.656	0
FAQ	663	3.8 (5.8)	5.6 (6.9) [a]	9.9 (8.5) [a,b]	<0.001	0.07
ApoE ε4, % carriers	1011	43	48	52	0.183	0
CSF biomarkers						
$Aß_{1-42}$ (pg/mL)	345	176.4 (59.1)	161.2 (49.4)	158.9 (53.6)	0.036	0.02
T-tau (pg/mL)	345	95.1 (53.3)	96.0 (54.5)	98.3 (54.5)	0.946	0
p-tau (pg/mL)	342	31.7 (16.9)	35.8 (20.4)	32.9 (16.2)	0.160	0.01
Cognitive variables						
TMT-A	664	44.5 (26.1)	48.5 (25.9)	58.7 (30.5) [a,b]	0.001	0.02
TMT-B	656	118.3 (72.5)	143.4 (81.7) [a]	173.8 (81.2) [a,b]	<0.001	0.05
Digit Symbol	662	40.0 (13.3)	35.4 (12.3) [a]	30.0 (11.7) [a,b]	<0.001	0.06
Digit span forward	665	8.3 (2.1)	8.1 (2.0)	8.2 (2.0)	0.664	0
Digit span backward	661	6.3 (2.3)	6.2 (2.1)	5.4 (1.6) [a]	0.014	0.01
Semantic fluency	665	17.1 (5.8)	15.9 (5.6) [a]	13.5 (5.7) [a,b]	<0.001	0.03
AVLT learning	661	34.9 (11.1)	31.2 (10.9) [a]	26.0 (10.5) [a,b]	<0.001	0.06
AVLT delayed	664	4.2 (4.1)	3.4 (4.1) [a]	2.0 (2.8) [a]	<0.001	0.03
AVLT recognition	664	10.5 (3.9)	9.8 (4.3)	9.2 (4.4)	0.027	0.01
BNT	660	26.2 (4.5)	25.1 (4.8) [a]	23.4 (5.9) [a,b]	<0.001	0.03
Clock test	665	4.3 (1.0)	4.0 (1.1) [a]	3.7 (1.3) [a,b]	<0.001	0.03
Memory Clinic						
MMSE	32	23.4 (7.0)	18.0 (9.5)	21.0 (7.3)	0.308	0.08

Data on clinical status, CSF biomarkers, and cognition were available for 1023, 345, and 665 participants, respectively (AddNeuroMed and ADNI samples). [a] significantly different from GCA-F=0; [b] significantly different from GCA-F=1; Values in the table represent mean (standard deviation); Bonferroni correction for five comparisons (ANOVA for clinical variables): $p \leq 0.010$; Bonferroni correction for three comparisons (ANOVA for CSF biomarkers): $p \leq 0.017$; Bonferroni correction for eleven comparisons (ANOVA for cognitive variables): $p \leq 0.005$; All post-hoc analyses were also adjusted using Bonferroni correction for multiple comparisons; GCA-F=global cerebral atrophy – frontal sub-scale; η_p^2 =partial eta squared; MMSE=Mini-Mental State Examination; CDR=Clinical Dementia Rating; GDS=geriatric depression scale; FAQ=functional activity questionnaire; $Aß_{1-42}$=amyloid-ß-peptide 1-42; T-tau=total level of tau protein; p-tau=level of phosphorylated tau protein; TMT=trail making test; AVLT=auditory verbal learning test; BNT=Boston naming test; pg/mL: picograms per millilitre

and GCA-F=2 extends investigation of disease severity. Another possible drawback is an inter-rater reliability of 0.59 (weighted kappa). However, agreement is almost substantial [41], and is superior to what was previously reported by the developers of the scale, with Fleiss' kappa values ranging from 0.29 to 0.48 (our Fleiss' kappa is 0.55) [11]. In addition, our intraclass correlation coefficient was optimal. Further, although a significant interaction was found indicating bvFTD patients having more frontal atrophy in the right hemisphere, and PNFA patients in the left hemisphere, this observation was only qualitative and together with absence of asymmetry in the SD subtype reflects limited statistical power due to the small sample size. Finally, GCA-F was applied in the axial plane as originally proposed by Pasquier et al. for the GCA scale [10]. Rating GCA-F in the three anatomical planes as proposed by the PA scale [7] might add some advantage and warrants future investigation.

In conclusion, GCA-F reliably reflects atrophy in the frontal lobe and shows associations with clinical and cognitive impairment. This scale may have implications for clinical practice as a supportive tool for disorders demonstrating predominant frontal atrophy such as FTD subtypes and the executive presentation of Alzheimer's disease. Future research is warranted to continue validating the GCA-F scale in these specific subgroups. GCA-F is simple, quick, and can be

performed both on magnetic resonance and computed tomography images. Due to this, we believe that GCA-F is feasible for use in clinical routine for the radiological assessment of dementia and other disorders.

Acknowledgments The scientific guarantor of this publication is Dr. Daniel Ferreira (Department of Neurobiology, Care Sciences and Society, Karolinska Institutet, Sweden). The authors of this manuscript declare no relationships with any companies, whose products or services may be related to the subject matter of the article. The authors thank Swedish Brain Power, the Strategic Research Programme in Neuroscience at Karolinska Institutet (StratNeuro), The Swedish Alzheimer Foundation, and the regional agreement on medical training and clinical research (ALF) between Stockholm County Council. AddNeuroMed is supported by InnoMed (Innovative Medicines in Europe), an Integrated Project funded by the European Union of the Sixth Framework programme priority FP6-2004-LIFESCIHEALTH-5, Life Sciences, Genomics and Biotechnology for Health. Data collection and sharing for the ADNI project was funded by the Alzheimer's Disease Neuroimaging Initiative (ADNI) (National Institutes of Health Grant U01 AG024904) and DOD ADNI (Department of Defense award number W81XWH-12-2-0012). ADNI is funded by the National Institute on Aging, the National Institute of Biomedical Imaging and Bioengineering, and through generous contributions from the following: Alzheimer's Association; Alzheimer's Drug Discovery Foundation; Araclon Biotech; BioClinica, Inc.; Biogen Idec Inc.; Bristol-Myers Squibb Company; Eisai Inc.; Elan Pharmaceuticals, Inc.; Eli Lilly and Company; EuroImmun; F. Hoffmann-La Roche Ltd and its affiliated company Genentech, Inc.; Fujirebio; GE Healthcare; IXICO Ltd.; Janssen Alzheimer Immunotherapy Research & Development, LLC.; Johnson & Johnson Pharmaceutical Research & Development LLC.; Medpace, Inc.; Merck & Co., Inc.; Meso Scale Diagnostics, LLC.; NeuroRx Research; Neurotrack Technologies; Novartis Pharmaceuticals Corporation; Pfizer Inc.; Piramal Imaging; Servier; Synarc Inc.; and Takeda Pharmaceutical Company. The Canadian Institutes of Health Research is providing funds to support ADNI clinical sites in Canada. Private sector contributions are facilitated by the Foundation for the National Institutes of Health (www.fnih.org). The grantee organization is the Northern California Institute for Research and Education, and the study is coordinated by the Alzheimer's Disease Cooperative Study at the University of California, San Diego. ADNI data are disseminated by the Laboratory for Neuro Imaging at the University of Southern California.

One of the authors has significant statistical expertise. Institutional Review Board approval was not required because this study includes data from AddNeuroMed and ADNI, two public and available datasets for imaging research. Data collection was subject to ethical review and approval by committees from each participating centre. This study also includes data from the Memory Clinic at Karolinska University Hospital. This sample has been previously investigated and the study was approved by the Regional Ethical Review Board in Stockholm, Sweden. Written informed consent was not required for this study because this study includes data from AddNeuroMed and ADNI, two public and available datasets for imaging research. Data collection was subject to ethical review and approval by committees from each participating center. This study also includes data from the Memory Clinic at Karolinska University Hospital. This sample has been previously investigated and written informed consent was already available for all the subjects. Some study subjects or cohorts have been previously reported. Data from the AddNeuromed and the ADNI studies have been extensively used and reported. Given the amount of manuscript published using these two datasets, it is not possible to mention the number of patients previously published. This study also includes data from thirty-four patients previously investigated in the studies listed below.

- Looi et al. AJNR Am J Neuroradiol 2008
- Lindberg et al. AJNR Am J Neuroradiol 2009
- Looi et al. AJNR Am J Neuroradiol 2009
- Looi et al. Neuroimage 2010
- Looi et al. Psychiatry Res 2011
- Lindberg et al. J Alzheimers Dis 2012
- Lindberg et al. AJNR Am J Neuroradiol 2012
- Lindberg et al. Front Aging Neurosci 2012
- Walterfang et al. J Alzheimers Dis 2014

Methodology: prospective, cross sectional study, multicenter study.

Appendix

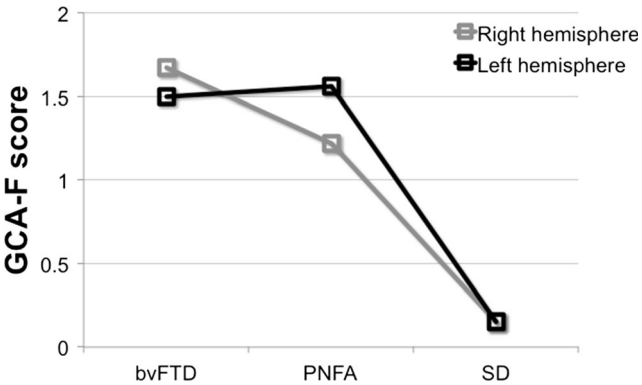

Fig. 5 Interaction between FTD subtype and hemisphere. GCA-F= global cerebral atrophy – frontal sub-scale; bvFTD=behavioural variant of frontotemporal dementia; SD=semantic dementia; PNFA=progressive non-fluent aphasia

Table 6 FreeSurfer 5.3.0 methods for cortical reconstruction and parcellation

1) Motion correction [56].
2) Removal of non-brain tissue [57].
3) Automated Talairach transformation.
4) Segmentation of the subcortical structures [51, 52].
5) Intensity normalization [59].
6) Tessellation of the gray matter white matter boundary.
7) Automated topology correction [50, 58].
8) Surface deformation following intensity gradients to optimally place the gray/white and gray/cerebrospinal fluid borders at the location where the greatest shift in intensity defines the transition to the other tissue class [43, 44, 49].
9) Surface inflation [47], registration to a spherical atlas [48].
10) Parcellation of the cerebral cortex into units based on gyral and sulcal structure [45, 53].
11) Creation of a variety of surface based data.

Table 7 Detailed methods for manual tracing of frontal sub-regions

1) The software program MRIcro (http://www.mccauslandcenter.sc.edu/mricro/) was used for parcellation of the cortex. Measurements were subsequently performed on the HERMES MultiModality software package (Nuclear Diagnostics, Stockholm Sweden).
2) Regions of interest were traced manually on contiguous coronal sections including the following areas:
- Superior frontal gyrus (SFG) (Brodmann areas 6, 8, 9, and 32).
- Middle frontal gyrus (MFG) (Brodmann area 46).
- Inferior frontal gyrus (IFG) (Brodmann areas 44 and 45).
- Orbitofrontal cortex (ORB) (Brodmann areas 10, 11, 12, and 47).
- Dorsal anterior cingulate gyrus (DACC) (Brodmann area 24).

The following established protocols were used for parcellation of SFG, MFG, IFG and ORB [42] and for DACC [55]). For the posterior border of the DACC, the protocol by Fornito et al [54] was preferred, stopping tracing one section after the disappearance of the anterior commissure, moving from anterior to posterior on coronal sections.
3) Following the landmarks proposed by Eritaia et al. [46], the total intracranial volume (TIV) was obtained using a stereology-based technique on every fourth section of the brain,
4) All regional volumes were then normalized by the TIV (regional volume / TIV).
5) All volumetric data were obtained by O.L., who was completely blind to clinical data. The intraclass correlation coefficient on ten repeated measurements (at least one month apart) was over 0.90. Inter-rater reliability was not calculated but the delineation of each region on approximately ten brains was scrutinized and approved by an experienced neuroanatomist.

Table 8 Demographic characteristics of the three GCA-F groups

AddNeuroMed+ADNI, *n*	GCA-F=0 536	GCA-F=1 399	GCA-F=2 101	*p* -
Age, mean (Sd)	73.4 (6.3)	76.9 (6.1) [a]	78.1 (6.3) [a]	<0.001
Gender, % female	52	42	40	0.003
Years of education, mean (Sd) [1]	14.0 (4.4)	12.9 (5.0) [a]	12.8 (4.8) [a]	0.001
Diagnosis. HC, *n* (%)	210 (39)	107 (27)	12 (12)	<0.001
MCI, *n* (%)	220 (41)	163 (41)	38 (38)	
AD, *n* (%)	106 (20)	129 (32)	51 (50) [*]	
Memory Clinic, *n*	12	11	11	
Age, mean (Sd)	63.7 (7.4)	63.2 (7.4)	60.6 (7.3)	0.560
Gender, % female	58	73	73	0.813
Years of education, mean (Sd) [2]	11.6 (3.2)	9.6 (3.7)	11.0 (2.6)	0.376
Diagnosis. bvFTD, *n* (%)	1 (8)	3 (27)	8 (73) [*]	<0.001
PNFA, *n* (%)	0 (0)	6 (55)	3 (27) [*]	
SD, *n* (%)	11 (92)	2 (18)	0 (0)	

[1] $n=1033$; [2] $n=28$; [*] One AD patient, one bvFTD patient, and one PNFA patient rated as GCA-F=3 were added to the GCA-F=2 group in order to provide three large GCA-F groups. [a] significantly different from GCA-F=0; [b] significantly different from GCA-F=1; Bonferroni correction for four comparisons: $p \leq 0.013$; All post-hoc analyses were also adjusted using Bonferroni correction for multiple comparisons; GCA-F=global cerebral atrophy – frontal sub-scale; Sd=standard deviation; HC=healthy controls; MCI=mild cognitive impairment; AD=Alzheimer's disease; FTD=frontotemporal dementia; bvFTD=behavioural variant of frontotemporal dementia; PNFA=progressive non-fluent aphasia; SD=semantic dementia

Table 9 Summary of significant clusters in analyses at the vertex level (AddNeuroMed+ADNI)

Comparison			MNI coordinates			Location of cluster maxima
Marker, hemisphere	Cluster	Size (mm^2)	*x*	*y*	*z*	
GCA-F=0 *vs.* GCA-F=1 (*n*=935)						
Volume, left	Cluster 1	57489	-36.8	-18.3	64.5	precentral
Volume, right	Cluster 1	57141	30.6	-47.5	44.4	superior parietal
Thickness, left	Cluster 1	66410	-11.5	-7.7	47.3	superior frontal
Thickness, right	Cluster 1	68818	27.7	-14.4	60.2	precentral
Area, left	Cluster 1	15623	-53.1	-24	-4	superior temporal
	Cluster 2	7166	-11.5	-7.7	47.3	superior temporal
	Cluster 3	2775	-7.8	-72.8	46.2	precuneus
	Cluster 4	2150	-49.6	-48	44.6	supramarginal
Area, right	Cluster 1	18487	45.9	-43.8	7.5	temporal banks
	Cluster 2	3337	27.7	57.8	-9.5	rostral middle frontal
	Cluster 3	2647	9.4	-50.8	47.8	precuneus
GCA-F=1 *vs.* GCA-F=2 (*n*=500)						
Volume, left	Cluster 1	18058	-49.6	-48	44.6	supramarginal
	Cluster 2	15682	-22.1	41.5	24.1	rostral middle frontal
	Cluster 3	1485	-37.6	15.5	9.8	pars opercularis
	Cluster 4	1272	-12	-67.1	34.7	precuneus
Volume, right	Cluster 1	34784	38.7	41	24	rostral middle frontal
	Cluster 2	3141	34	-71.1	28.7	inferior parietal
Thickness, left	Cluster 1	35680	-22.1	41.5	24.1	rostral middle frontal
		2037	-12	-67.1	34.7	precuneus
Thickness, right	Cluster 1	38308	38.7	41	24	rostral middle frontal
Area, left	Cluster 1	10157	-53.1	-24	-4	superior temporal
	Cluster 2	4241	-12.5	53.1	3.1	superior frontal
	Cluster 3	1828	-15.1	-78.4	10.8	pericalcarine
	Cluster 4	1640	-16.5	-45.3	54.7	precuneus
Area, right	Cluster 1	11106	21.3	-98.7	5.3	lateral occipital
	Cluster 2	5928	13.8	22.4	30.5	superior frontal
	Cluster 3	1800	45.9	-43.8	7.5	temporal banks

GCA-F=global cerebral atrophy – frontal sub-scale; MNI=Montreal Neurological Institute

References

1. McKhann GM, Knopman DS, Chertkow H et al (2011) The diagnosis of dementia due to Alzheimer's disease: recommendations from the National Institute on Aging-Alzheimer's Association workgroups on diagnostic guidelines for Alzheimer's disease. Alzheimers Dement 7:263–269
2. Scheltens P, Leys D, Barkhof F et al (1992) Atrophy of medial temporal lobes on MRI in "probable" Alzheimer's disease and normal ageing: diagnostic value and neuropsychological correlates. J Neurol Neurosurg Psychiatry 55:967–972
3. Dubois B, Feldman HH, Jacova C et al (2007) Research criteria for the diagnosis of Alzheimer's disease: revising the NINCDS-ADRDA criteria. Lancet Neurol 6:734–746
4. Shim YS, Youn YC, Na DL et al (2011) Effects of medial temporal atrophy and white matter hyperintensities on the cognitive functions in patients with Alzheimer's disease. Eur Neurol 66:75–82
5. Scheltens P, Fox N, Barkhof F, De Carli C (2002) Structural magnetic resonance imaging in the practical assessment of dementia: beyond exclusion. Lancet Neurol 1:13–21

6. Deweer B, Lehericy S, Pillon B et al (1995) Memory disorders in probable Alzheimer's disease: the role of hippocampal atrophy as shown with MRI. J Neurol Neurosurg Psychiatry 58:590–597
7. Koedam EL, Lehmann M, van der Flier WM et al (2011) Visual assessment of posterior atrophy development of a MRI rating scale. Eur Radiol 21:2618–2625
8. Lehmann M, Koedam EL, Barnes J et al (2012) Posterior cerebral atrophy in the absence of medial temporal lobe atrophy in pathologically-confirmed Alzheimer's disease. Neurobiol Aging 33:627.e1–627.e12
9. Elliott R (2003) Executive functions and their disorders. Br Med Bull 65:49–59
10. Pasquier F, Leys D, Weerts JG, Mounier-Vehier F, Barkhof F, Scheltens P (1996) Inter-and intraobserver reproducibility of cerebral atrophy assessment on MRI scans with hemispheric infarcts. Eur Neurol 36:268–272
11. Scheltens P, Pasquier F, Weerts JG, Barkhof F, Leys D (1997) Qualitative assessment of cerebral atrophy on MRI: inter- and intra-observer reproducibility in dementia and normal aging. Eur Neurol 37:95–99
12. Henneman WJP, Vrenken H, Barnes J et al (2009) Baseline CSF p-tau levels independently predict progression of hippocampal atrophy in Alzheimer disease. Neurology 73:935–940
13. Van der Vlies AE, Goos JDC, Barkhof F, Scheltens P, van der Flier WM (2012) Microbleeds do not affect rate of cognitive decline in Alzheimer disease. Neurology 79:763–769
14. Doody RS, Azher SN, Haykal HA, Dunn JK, Liao T, Schneider L (2000) Does APO 4 correlate with MRI changes in Alzheimer's disease? J Neurol Neurosurg Psychiatry 69:668–671
15. Biessels GJ, De Leeuw F-E, Lindeboom J, Barkhof F, Scheltens P (2006) Increased cortical atrophy in patients with Alzheimer's disease and type 2 diabetes mellitus. J Neurol Neurosurg Psychiatry 77:304–307
16. Goos JDC, Kester MI, Barkhof F et al (2009) Patients with Alzheimer disease with multiple microbleeds: relation with cerebrospinal fluid biomarkers and cognition. Stroke 40:3455–3460
17. Kim Y-S, Lee K-M, Choi BH, Sohn EH, Lee AY (2009) Relation between the clock drawing test (CDT) and structural changes of brain in dementia. Arch Gerontol Geriatr 48:218–221
18. Ferreira D, Cavallin L, Larsson E-M, et al. (2015) Practical cut-offs for visual rating scales of medial temporal, frontal, and posterior atrophy in Alzheimer's disease and mild cognitive impairment. J Intern Med 278:277–290
19. Möller C, van der Flier WM, Versteeg A et al (2014) Quantitative regional validation of the visual rating scale for posterior cortical atrophy. Eur Radiol 24:397–404
20. Bresciani L, Rossi R, Testa C et al (2005) Visual assessment of medial temporal atrophy on MR films in Alzheimer's disease: comparison with volumetry. Aging Clin Exp Res 17:8–13
21. Davies RR, Scahill VL, Graham A, Williams GB, Graham KS, Hodges JR (2009) Development of an MRI rating scale for multiple brain regions: comparison with volumetrics and with voxel-based morphometry. Neuroradiology 51:491–503
22. Simmons A, Westman E, Muehlboeck S et al (2011) The AddNeuroMed framework for multi-centre MRI assessment of Alzheimer's disease: experience from the first 24 months. Int J Geriatr Psychiatry 26:75–82
23. Mueller SG, Weiner MW, Thal LJ et al (2005) Ways toward an early diagnosis in Alzheimer's disease: The Alzheimer's Disease Neuroimaging Initiative (ADNI). Alzheimers Dement 1:55–66
24. Petersen RC, Aisen PS, Beckett LA et al (2010) Alzheimer's Disease Neuroimaging Initiative (ADNI): clinical characterization. Neurology 74:201–209
25. Lindberg O, Östberg P, Zandbelt BB, et al. (2009) Cortical morphometric subclassification of frontotemporal lobar degeneration. Am J Neuroradiol 30:1233–1239
26. Neary D, Snowden J, Gustafson L et al (1998) Frontotemporal lobar degeneration: a consensus on clinical diagnostic criteria. Neurology 51:1546–1554
27. Jack CR, Bernstein MA, Fox NC et al (2008) The Alzheimer's Disease Neuroimaging Initiative (ADNI): MRI methods. J Magn Reson Imaging 27:685–691
28. Liu Y, Paajanen T, Zhang Y et al (2011) Combination analysis of neuropsychological tests and structural MRI measures in differentiating AD, MCI and control groups–the AddNeuroMed study. Neurobiol Aging 32:1198–1206
29. Kipps CM, Davies RR, Mitchell J, Kril JJ, Halliday GM, Hodges JR (2007) Clinical significance of lobar atrophy in frontotemporal dementia: application of an MRI visual rating scale. Dement Geriatr Cogn Disord 23:334–342
30. Victoroff J, Mack W, Grafton S, Schreiber SS, Chui HC (1994) A method to improve interrater reliability of visual inspection of brain MRI scans in dementia. Neurology 44:2267–2276
31. Ferreira D, Molina Y, Machado A et al (2014) Cognitive decline is mediated by gray matter changes during middle age. Neurobiol Aging 35:1086–1094
32. Dickerson BC, Feczko E, Augustinack JC et al (2009) Differential effects of aging and Alzheimer's disease on medial temporal lobe cortical thickness and surface area. Neurobiol Aging 30:432–440
33. Nygaard GO, Walhovd KB, Sowa P et al (2014) Cortical thickness and surface area relate to specific symptoms in early relapsing-remitting multiple sclerosis. Mult Scler 21:402–414
34. Jubault T, Gagnon J-F, Karama S et al (2011) Patterns of cortical thickness and surface area in early Parkinson's disease. Neuroimage 55:462–467
35. Meda SA, Pryweller JR, Thornton-Wells TA (2012) Regional brain differences in cortical thickness, surface area and subcortical volume in individuals with Williams syndrome. PLoS One 7, e31913
36. Rimol LM, Nesvåg R, Hagler DJ et al (2012) Cortical volume, surface area, and thickness in schizophrenia and bipolar disorder. Biol Psychiatry 71:552–560
37. Miller B, Chang L, Mena I, Boone K, Lesser IM (1993) Progressive right frontotemporal degeneration: clinical, neuropsychological and SPECT characteristics. Dementia 4:204–213
38. Grossman M, McMillan C, Moore P et al (2004) What's in a name: voxel-based morphometric analyses of MRI and naming difficulty in Alzheimer's disease, frontotemporal dementia and corticobasal degeneration. Brain 127:628–649
39. Lindberg O, Manzouri A, Westman E, Wahlund LO (2012) A comparison between volumetric data generated by voxel-based morphometry and manual parcellation of multimodal regions of the frontal lobe. Am J Neuroradiol 33:1957–1963
40. Whitwell JL, Jack CR (2005) Comparisons between Alzheimer disease, frontotemporal lobar degeneration, and normal aging with brain mapping. Top Magn Reson Imaging 16:409–425
41. Landis J, Koch G (1977) The measurement of observer agreement for categorical data. Biometrics 33:159–174
42. Crespo-Facorro B, Kim J, Andreasen NC et al (2000) Cerebral cortex: a topographic segmentation method using magnetic resonance imaging. Psychiatry Res 100:97–126
43. Dale AM, Sereno MI (1993) Improved localization of cortical activity by combining EEG and MEG with MRI cortical surface reconstruction: a linear approach. J Cogn Neurosci 5:162–176
44. Dale AM, Fischl B, Sereno MI (1999) Cortical surface-based analysis i: segmentation and surface reconstruction. NeuroImage 9: 179–194
45. Desikan RS, Ségonne F, Fischl B et al (2006) An automated labeling system for subdividing the human cerebral cortex on MRI scans into gyral based regions of interest. NeuroImage 31:968–980

46. Eritaia J, Wood SJ, Stewart GW et al (2000) An optimized method for estimating intracranial volume from magnetic resonance images. Magn Reson Med 44:973–977
47. Fischl B, Sereno MI, Dale AM (1999) Cortical surface-based analysis. II: inflation, flattening, and a surface-based coordinate system. NeuroImage 9:195–207
48. Fischl B, Sereno MI, Tootell RB, Dale AM (1999) High-resolution inter-subject averaging and a coordinate system for the cortical surface. Hum Brain Mapp 8:272–284
49. Fischl B, Dale AM (2000) Measuring the thickness of the human cerebral cortex from magnetic resonance images. Proc Natl Acad Sci U S A 97:11050–11055
50. Fischl B, Liu A, Dale AM (2001) Automated manifold surgery: constructing geometrically accurate and topologically correct models of the human cerebral cortex. IEEE Trans Med Imaging 20:70–80
51. Fischl B, Salat DH, Busa E et al (2002) Whole brain segmentation: automated labeling of neuroanatomical structures in the human brain. Neuron 33:341–355
52. Fischl B, Salat DH, Van der Kouwe AJW et al (2004) Sequence-independent segmentation of magnetic resonance images. NeuroImage 23(Suppl 1):S69–S84
53. Fischl B, van der Kouwe A, Destrieux C et al (2004) Automatically parcellating the human cerebral cortex. Cereb Cortex 14:11–22
54. Fornito A, Whittle S, Wood SJ, Velakoulis D, Pantelis C, Yücel M (2006) The influence of sulcal variability on morphometry of the human anterior cingulate and paracingulate cortex. NeuroImage 33: 843–854
55. McCormick LM, Ziebell S, Nopoulos P, Cassell M, Andreasen NC, Brumm M (2006) Anterior cingulate cortex: an MRI-based parcellation method. NeuroImage 32:1167–1175
56. Reuter M, Rosas HD, Fischl B (2010) Highly accurate inverse consistent registration: a robust approach. NeuroImage 53:1181–1196
57. Ségonne F, Dale AM, Busa E et al (2004) A hybrid approach to the skull stripping problem in MRI. NeuroImage 22:1060–1075
58. Ségonne F, Pacheco J, Fischl B (2007) Geometrically accurate topology-correction of cortical surfaces using nonseparating loops. IEEE Trans Med Imaging 26:518–529
59. Sled JG, Zijdenbos AP, Evans AC (1998) A nonparametric method for automatic correction of intensity nonuniformity in MRI data. IEEE Trans Med Imaging 17:87–97